Modeling of Electromagnetic Scattering from Simplified Leaf Structures by Using Spherical Wave Expansion

Paul Jason Co and Jun-Ichi Takada
Department of International Development Engineering, Tokyo Institute of Technology, Tokyo, Japan

Abstract— Leaf scatterers are a type of obstacle that is abundant in rural propagation environments. These leaf scatterers interact with propagating radio waves which may affect the performance of wireless systems operating in such environments. In this paper, deciduous leaf scatterers are modelled as thin dielectric disks. The electromagnetic scattering from these disks at 2 GHz are modelled using the generalised Rayleigh-Gans (GRG) approximation as well as using a commercial method of moment (MoM) solver. The difference between the GRG and MoM results for the single scatterer case is evaluated using the spherical wave expansion of the scattered fields from both methods. An approximation of the scattered fields for the multiple scatterer scenario based on the superposition of the GRG scattered fields is presented and is compared to MoM results.

1. INTRODUCTION

Foliage structures are one of the most dominant types of obstacles that are present in rural propagation environments. These foliage obstacles, composed of leaves, branches and trunks act as complex scatterers to propagating radio waves in such environments. This interaction between the propagating radio waves and the foliage obstacles may significantly affect the performance of radio systems operating in such environments. The proper understanding of such interactions is necessary to predict their effects on radio systems. The complex and random nature of these foliage structures provide a significant challenge in predicting their effects on these propagating radio waves.

One element that makes up these foliage obstacle are their leaf structures. These leaf geometries are generally complex, which makes it difficult to find an exact solution to their scattered fields. One approach to approximate the scattered fields from such leaf structures is to represent these leaf structures as thin dielectric disks for deciduous trees, and as thin dielectric cylinders for coniferous trees [1–3]. Approximate analytical solutions may be used to evaluate the scattered fields from these simplified leaf geometries [4]. In this paper, we take a look at the generalised Rayleigh-Gans approximation and make use of the spherical wave expansion to compare the scattering with a method of moment (MoM) solution. The scattering from multiple simplified leaf structures using the superposition of the GRG approximation is also compared to the numerical results.

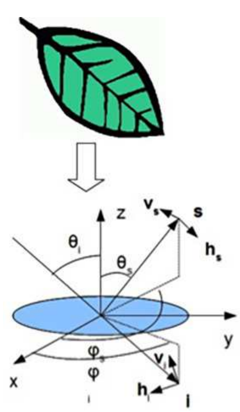

Figure 1: Simplified leaf geometry.

2. SINGLE SCATTERER

The simplified scattering geometry for deciduous leaves is illustrated in Figure 1. The deciduous leaf is modelled as a thin dielectric disk centered at the origin on the x-y plane, with radius R, thickness t, and relative permittivity ϵ_r. The disk is illuminated by a uniform plane wave given by Equation (1), where k is the wave number $\mathbf{i}$ is the direction of incidence, $\mathbf{r}$ is the position vector of the point of interest, and $\mathbf{q} = \mathbf{v_i}$ or $\mathbf{h_i}$ are the unit vectors defining the polarization of the incident wave, where $\mathbf{h}$ is perpendicular to the direction of propagation and the z axis, and $\mathbf{v}$ is perpendicular to the direction of propagation and $\mathbf{h}$ as defined in [2].

$$\vec{E}_i = \mathbf{q}E_0 e^{-jk\mathbf{i}\cdot\mathbf{r}} \tag{1}$$

$$\mathbf{i} = \sin\theta_i(\mathbf{x}\cos\phi_i + \mathbf{y}\sin\phi_i) - \mathbf{z}\cos\theta_i \tag{2}$$

$$\mathbf{h_i} = \frac{\mathbf{z}\times\mathbf{i}}{|\mathbf{z}\times\mathbf{i}|} \tag{3}$$

$$\mathbf{v_i} = \mathbf{h_i}\times\mathbf{i} \tag{4}$$

The generalised Rayleigh-Gans approximation approximates the scattered fields from small scatterers in which one dimension is much smaller than the other dimensions of the scatterer. The scattered fields are dependent on the geometry of the scatterer as well as its electrical properties. The scattered fields in the direction $\mathbf{s}$ due to an incident plane wave in the direction of $\mathbf{i}$ approximated by the GRG approximation can be expressed as:

$$\vec{E_S}(\mathbf{s},\mathbf{i}) = \bar{\bar{F}}(\mathbf{s},\mathbf{i})\cdot\mathbf{q}E_0\frac{e^{-jkr}}{r} \tag{5}$$

The scattering amplitude tensor $\bar{\bar{F}}(\mathbf{s},\mathbf{i})$ is as in [2].

We apply the GRG approximation to the geometry in Figure 1 with thickness of 0.1 mm and radius of 1.5 cm, with incident plane waves with a magnitude of 1, and incident angles of $0 \leq \theta_i \leq 180°$, with polarisations of either $\mathbf{v_i} = 1$, $\mathbf{h_i} = 0$ or $\mathbf{v_i} = 0$, $\mathbf{h_i} = 1$. The scattered fields from the same geometries are evaluated numerically using FEKO, a commercial method of moments solver. The scattered fields from the disk for an incident angle of $\theta_i = 45°$ is shown in Figure 2 for both the GRG approximation and the MoM solution. We express the error between the numerical and GRG scattered field magnitudes as:

$$\text{error\%} = \frac{\left|\left|\vec{E}_{\mathrm{S}}^{\mathrm{MoM}}(\mathbf{s},\mathbf{i})\right| - \left|\vec{E}_{\mathrm{S}}^{\mathrm{GRG}}(\mathbf{s},\mathbf{i})\right|\right|}{\left|E_{\mathrm{S}}^{\vec{\mathrm{MoM}}}(\mathbf{s},\mathbf{i})\right|}\times 100\% \tag{6}$$

For the vertically polarised incident wave, the average error over all scattering directions for $0 \leq \theta_i \leq 180°$ was found to be approximately 1.24%. Similarly, for the horizontally polarised incident wave, the average error was found to be approximately 3.28%. Further inspection of the average error for various incidence angles is shown in Figure 3. It can be seen that the error increases as the incidence angle approaches $\theta_i = 90°$ for both polarisation cases, with the h polarized incident wave having a larger error.

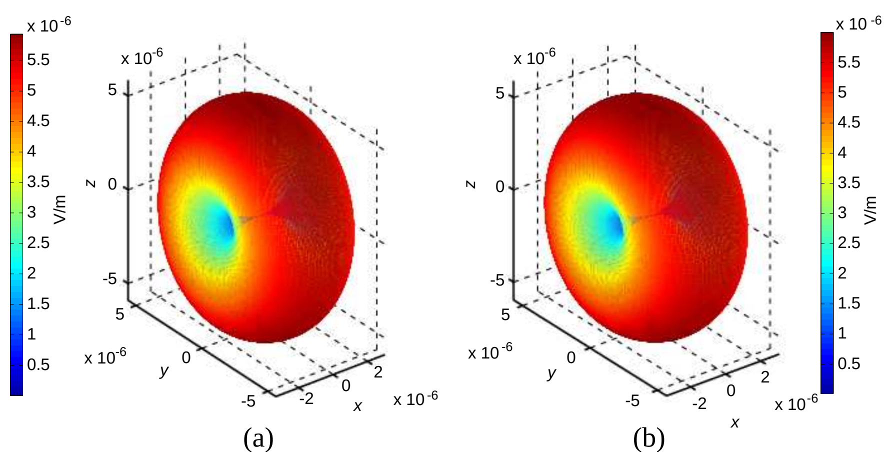

Figure 2: Scattered fields from (a) GRG and (b) MoM with $\theta_i = 45°$.

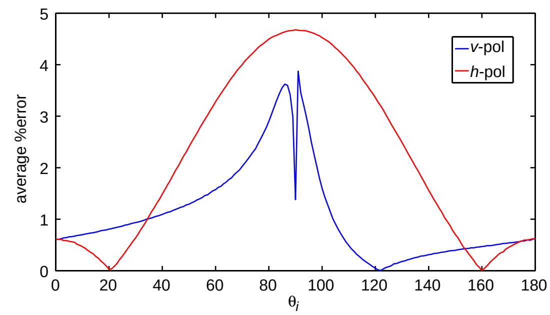

Figure 3: Average percentage error of scattered field magnitudes between MoM and GRG for varying incidence angles.

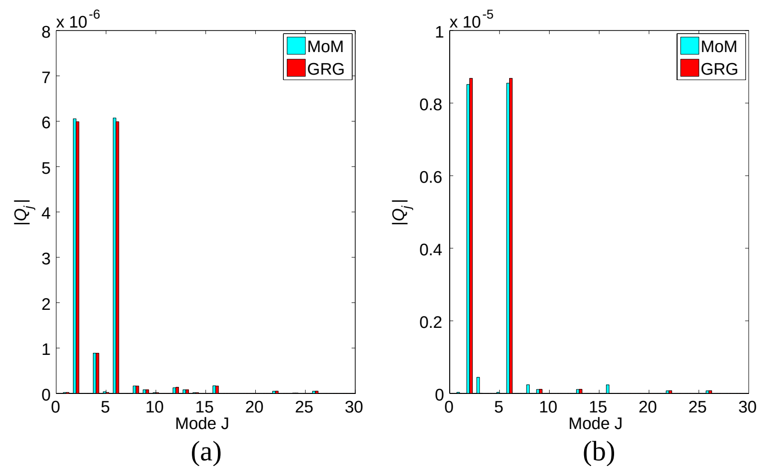

Figure 4: Spherical wave expansion coefficients of scattered fields for $\theta_i = 45°$; (a) v polarised and (b) h polarized.

Spherical wave expansion was used to gain more insight on the difference of the scattered fields evaluated. The spherical wave expansion of outward traveling waves can be expressed as [5].

$$\vec{E_S}(\mathbf{r}) = \frac{k}{\sqrt{\eta}} \sum_{j=1}^{J} Q_j(\mathbf{i}, \mathbf{q}) \vec{F}_j^{(4)}(\mathbf{r}) \tag{7}$$

$Q_j(\mathbf{i}, \mathbf{q})$ are the spherical wave coefficients and $\vec{F}_j(\mathbf{r})$ are the associated spherical wave functions defined in [5]. The spherical wave coefficients are evaluated via point matching from the evaluated scattered fields from the GRG and MoM solutions. The spherical wave expansions are truncated to $J = 30$ spherical modes as further increasing of the mode expansion does not yield any significant improvement of the expansion. Figure 4 illustrates the spherical wave expansion coefficients for an incident angle of $\theta_i = 45°$ for both v and h polarised incident waves. It can be seen from the figure that both MoM and GRG results have the same dominant modes, with small discrepancies in the magnitudes of these modes. It can also be seen that there is larger discrepancy in the h polarised incident waves. Evaluating the average error between the MoM and GRG coefficients over all incidence angles for each expansion coefficient results in Figure 5. For h polarised incident waves, we find that there is a larger error in the coefficients between the MoM and GRG results, which agrees with the results in the evaluation of the errors in the field scattering amplitudes that there is larger discrepancy in the MoM and GRG solutions for h polarised incident waves. Evaluation of the total scattered power from the spherical wave expansion using (8) [5] yields the average total scattered power tabulated in Table 1. The results show that the GRG and MoM solutions have very good agreement, with the GRG approximation underestimating the scattered fields by a small amount when the incident wave is v polarised, and overestimating the scattered fields when the

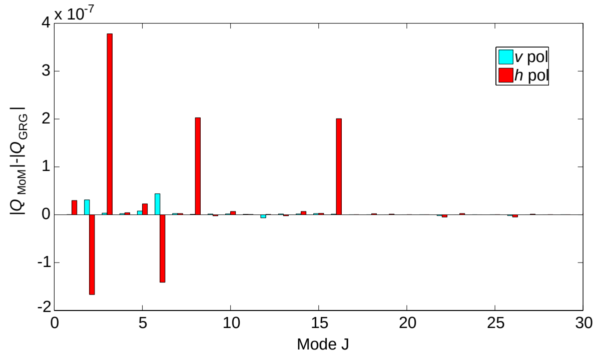

Figure 5: Average error of spherical wave coefficients.

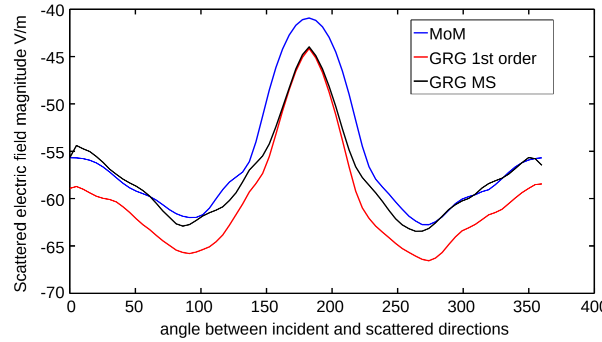

Figure 6: Scattered fields from multiple scatterers.

Table 1: Average total scattered power.

	v polarised incident wave	h polarised incident wave
MoM average total scattered power	-74.21 dBm	-71.37 dBm
GRG average total scattered power	-74.27 dBm	-71.23 dBm

incident wave is h polarised.

$$P_{\mathrm{S}} = \frac{1}{2}\sum_{j=1}^{J} |Q_j|^2 \tag{8}$$

3. MULTIPLE SCATTERERS

An approximation for multiple scatterers is presented by applying superposition to the GRG approximation. As a first approximation, the scattering from multiple leaf structures can be expressed as a superposition of the direct scattering from each individual scatterer evaluated from the GRG approximation. In terms of the scattered fields of a single scatterer, this total first order scattered fields from multiple scatterers can be expressed as:

$$\vec{E}_{\mathrm{S}}^{(1)} = \sum_{n=1}^{N} \vec{E}_{\mathrm{S},n} \tag{9}$$

where n is the index of scatterer in the volume of interest, and N is the total number of scatterers. For the second order approximation, we assume that the first order scattered fields from the scatterers in the volume of interest serve as the second order source to each of the other scatterers in the volume. Letting $\vec{E}_{S,m}$ be the second order scattered fields from scatterer m and $\vec{E}_{S,mn}$ be the scattered field from scatterer n incident to scatterer m, the scatterd fields in the point of interest $\mathbf{s}$ can be expressed as:

$$\vec{E}_{\mathrm{S},m} = \sum_{n=1, n\neq m}^{N} \bar{\bar{F}}_m \vec{E}_{\mathrm{S},mn} \tag{10}$$

$$\vec{E}_{\mathrm{S,Total}} = \vec{E}_{\mathrm{S}}^{(1)} + \sum_{m=1}^{N} \vec{E}_{\mathrm{S},m} \tag{11}$$

where the first term corresponds to the direct scattered fields, and the second term corresponds to the second order scattering that occurs in the volume. Figure 6 shows the average scattered fields of 30 realisations of 20 randomly positioned and oriented disk scatterers within a $0.5\,\mathrm{m} \times 0.5\,\mathrm{m} \times 0.5\,\mathrm{m}$ volume. The blue line corresponds to the numerical results, the red line corresponds to the first order superposition of the GRG approximation, and the black line corresponds to the second order approximation considering the second order scattering. We find that without multiple scattering, the GRG approximation underestimates the total scattered fields. Including the second order scattering improves the scattering magnitude in the back scattering direction, with minimal effect in the forward scattering direction.

4. CONCLUSION

The generalised Rayleigh-Gans approximation is considered to model the scattering from simplified leaf structures modelled as thin dielectric disks. The spherical wave expansion was used to describe the scattering from the GRG approximation and compare with a numerical method of moments solution. It was found that the GRG approximation has good agreement with the numerical results, with increasing error between the results in the region where θ_i approaches $90°$, with a horizontally polarised incident wave having a larger error. The superposition approximation of the scattered fields from multiple scatterers using GRG was shown, with second order scattering considered. The introduction of backscattering shows some improvement of the approximated scattering the the backward direction, with minimal effect in the forward direction. An extension of the single scatterer spherical wave expansion to evaluate the scattering from multiple scatterers will be done in the future.

REFERENCES

1. Schiffer, R. and K. O. Thielheim, "Light scattering by dielectric needles and disks," *Journal of Applied Physics*, Vol. 50, No. 4, 2476–2483, 1979.
2. Karam, M. A., A. K. Fung, and Y. M. M. Antar, "Electromagnetic wave scattering from some vegetation samples," *IEEE Trans. Geosci. Remote Sensing*, Vol. 26, No. 6, 799–808, 1988.
3. Karam, M. A. and A. K. Fung, "Leaf shape effects in electromagnetic scattering from vegetation," *IEEE Trans. Geosci. Remote Sensing*, Vol. 27, No. 6, 687–697, 1988.
4. Oh, Y. and J. Y. Hong, "Re-examination of analytical models for microwave scattering from deciduous leaves," *IET Microw. Antennas Propag.*, Vol. 1, No. 3, 617–623, 2007.
5. Hansen, J. E., *Spherical Near-field Measurements*, IEE Electromagnetic Wave Series 26, London UK, 1988.